The Dutch Apollo 11 Goodwill display contains genuine Moon rocks

Supplementary Information

S.1 Tomosynthesis

Tomosynthesis was performed on the Adaptix© XYP scanner at the University of Manchester. The setup is presented in Supplementary Figure 1 where the sample sits in the fixed space between the source and the detector in one of three positions. The GLSD was scanned upside down and on the side, providing radiographs with different viewing angles and varying amounts of wood and PMMA in the beam path. These scans used an acceleration voltage of 50 kV, and they were reconstructed in real-time with meshless reconstruction and artifact reduction tools [1, 2], providing initial information for further experimentation.

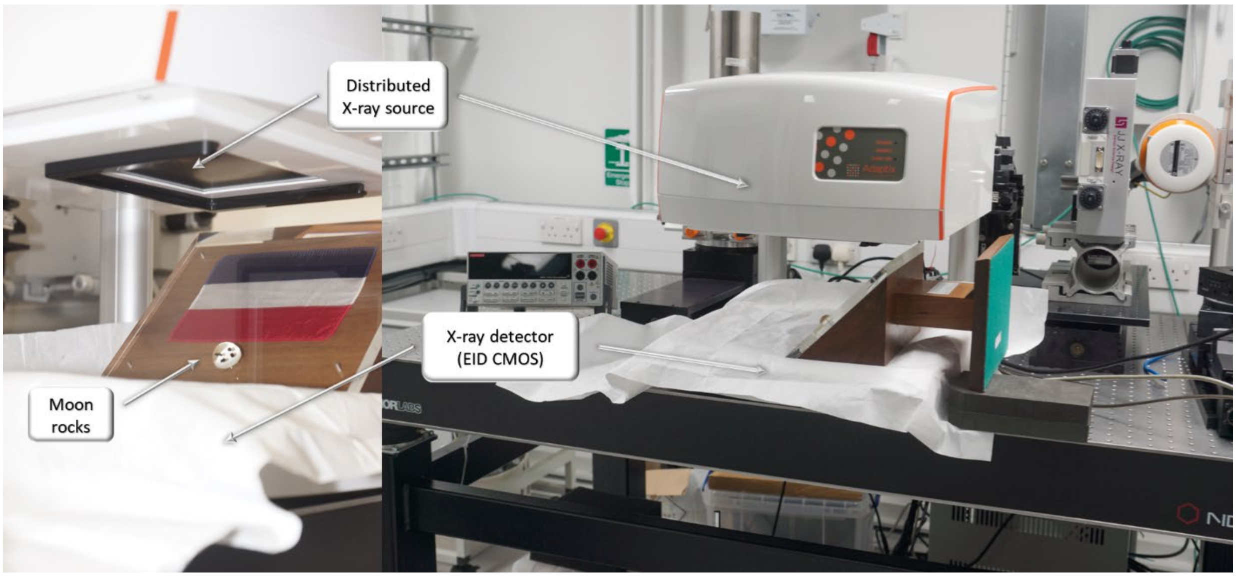

Supplementary Figure 1: Views of the tomosynthesis setup: close-up (left) and overall (right).

S.2 High-Resolution Microtomography

X-ray computed tomography was performed on a Zeiss Xradia 620 X-Ray Microscope (XRM). Two scans were acquired: a full volume of the dome and all four rocks inside (ScanA), and a high-resolution Region-of-Interest (ROI) acquisition (ScanB). The scan parameters are available in Supplementary Table 1.

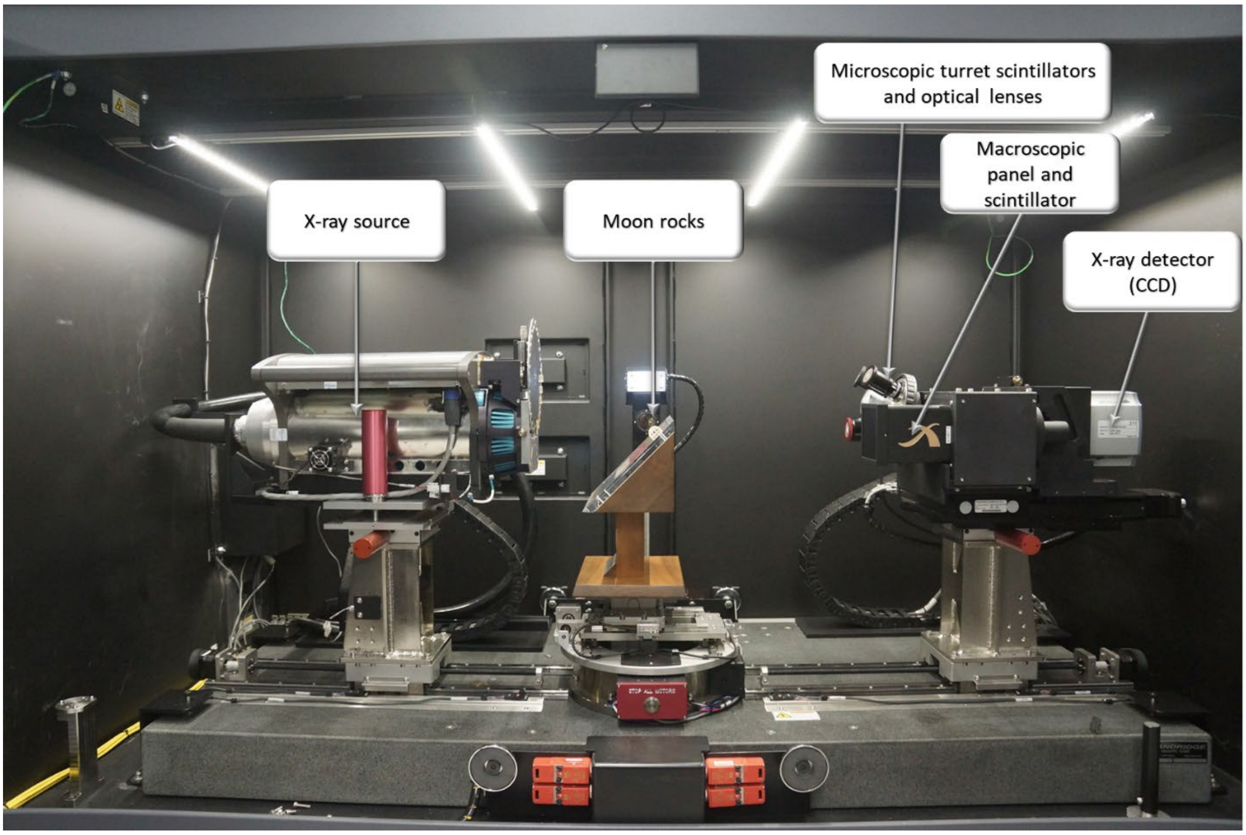

Supplementary Figure 2: Photography of object placed in the microtomography (XRM) setup.

The GLSD was attached to the sample stage with elastic bands. This was insufficient to prevent sample movement, which was further exacerbated by the position of the fragments a few dozen centimetres above the sample stage (Supplementary Figure 2). The pixel size was 22.27 μm for the macro tomography (Tomo-A) and 2.37 μm for the high-resolution tomography (Tomo-B). The transmission to absorption conversion for Tomo-B in Figure 5 is based on the Beer-Lambert Law. The XRM sample motion correction algorithm pre-stabilised the data before reconstruction, but the limited angle acquisition and remaining wobbling required further pre-processing and advanced reconstruction. For this work, we used the Core Imaging Library (CIL) toolbox [3], reordering the geometry for Astra [4], and applied motion correction, background correction, flat field calibration, padding, and other tools to improve the dataset. Reconstruction was performed with PDHG (Primal-Dual Hybrid Gradient) and explicit total variation with an alpha of 0.0005. Segmentation was performed in Avizo starting with a seed-propagation method to pre-segment the different phases, followed by a texture classification.

Supplementary Table 1: Information regarding tomography acquisitions on Zeiss Xradia Versa 620

	Tomo A	Tomo B
Pixel size (microns)	22.7	2.37
Acceleration (kV)	112.56	112.55
Number of images	1201	1201
Image dimensions	1024x1024	1012x1012
Binning	2	2
Source to RA distance (mm)	-151.55	-151.55
Detector to RA distance (mm)	314.34	273.88
Bits per pixel	16	16
Exposure time (s)	4	45

S.3 Hyperspectral X-ray Imaging

S.3.1 Hyperspectral Acquisition

Hyperspectral X-ray imaging was performed using a hybrid pixel photon counting detector based on the Timepix 3 ASIC (application-specific integrated circuit) developed by CERN and chip-bonded to a Cadmium Telluride 'CdTe' detector. This setup has a close to 100% energy sensitivity at 60 keV and an acceptable 3.6 keV energy resolution at 60 keV. This means that at the acceleration voltages used in the experiment, the sensor is equally efficient across the spectrum, and the resolution of a single peak Full Width Half Maximum (FWHM) σ at 60 keV is 3.6 keV and at 23 keV is 3.0 keV. Further, Timepix 3 is a direct readout (or clustering detector) processing every photon hit as it is received with a rate of up to 40 million hits per second and providing a precise event time and photon energy through Time-over-Threshold (ToT). The small size (14 x 14 mm) of the detector sitting on a fingerboard allowed it to be positioned in close proximity to the polyester hemisphere where the four moon rocks are encased. This had the advantage of maintaining sufficient detection efficiency. Rotating the sample stage also allowed different views to be obtained and, in coordination with the images obtained with the tomosynthesis scans, ensured that the rocks were not superimposing. Supplementary Figure 3 illustrates the setup with views of the X-ray source, which was set to operate at an acceleration voltage of 70 kV and a current of 14 μA, offering a moderate flux to allow the detector to keep up with data acquisition and avoid detector saturation.

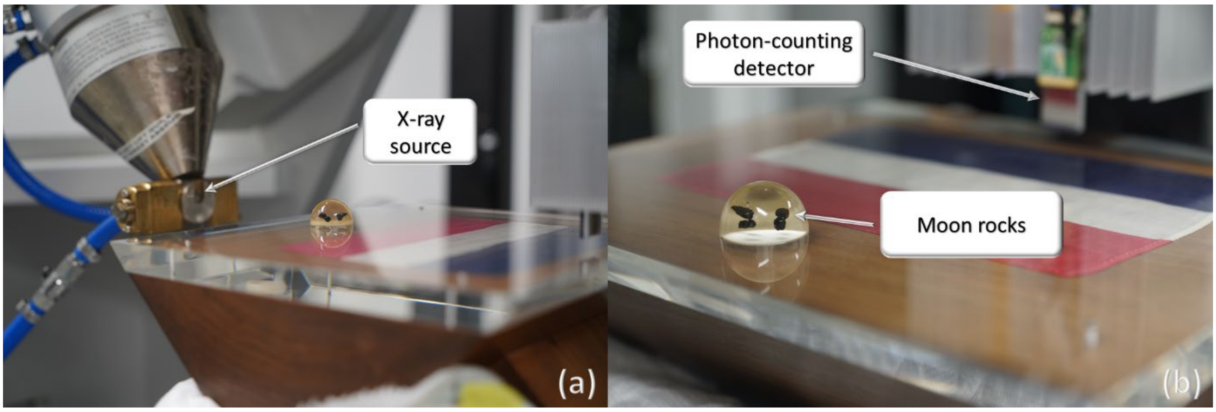

Supplementary Figure 3: Image of the hyperspectral imaging setup: towards the source (left) and the detector (right)

S.3.2 Hyperspectral Processing and Fitting

The Timepix 3 hyperspectral data was processed by reading the 'hit-list', which contains the impinging photon position on the 256 × 256 pixels grid as well as its energy, calibrated from ToT charge. It is then possible to define spectral bands, each containing pixel count and position information within an energy range. Here, each bin had a step size of 0.25 keV and a spread of 2.5 keV, meaning that a photon with energy 13.25 keV would be allocated to 4 different bins, each having a 0.25 keV step, helping to provide a higher signal-to-noise ratio. Supplementary Figure 4 presents the X-ray spectrum through a histogram of the mean pixel intensity on the Flat Field (no sample) image, as detected by the detector. Supplementary Figure 4b shows the integral image[1] which depicts the two fragments in the object of interest in the top right corner of the image. The dataset was corrected with a flat field to remove most camera defects, and a pixel correction mask was applied. Each spectral band was denoised with a 3D Gaussian filter with 1 standard deviation, and flat-field corrected to compensate for the variability of the spectrum from the source (as seen in

[1] This is an image formed by averaging all the data along the spectral dimension.

Supplementary Figure 4a). This was performed by choosing a Region of Interest (RoI) from the same dataset away from the sample but still going through the PMMA, which for uniform and large focal spot sources and small samples is a more efficient way to correct the spectrum. One may note that the K-edge of the tungsten target is at 69 keV, above what can be detected in the setup, and the cadmium and tellurium from the sensor material have been accounted for in the detector calibration. Supplementary Figure 5 presents side-by-side an integral and a colorized image, in which each point corresponds to a plot on the spectrum graph. The colour of the image is defined by selecting a range of energy bands, where the green colour signal comes out of the blue noise (Supplementary Figure 5).

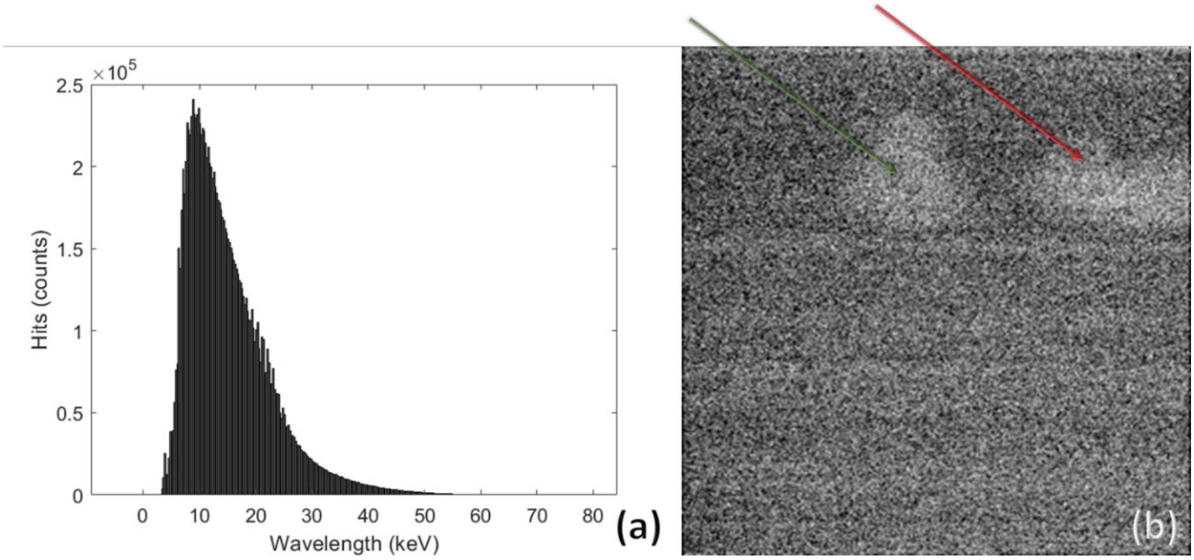

Supplementary Figure 4: Additional X-ray data: histogram of the open beam with no sample (a) and summed TOT-radiography (b) with arrows pointing at the Moon rocks 4 and 3

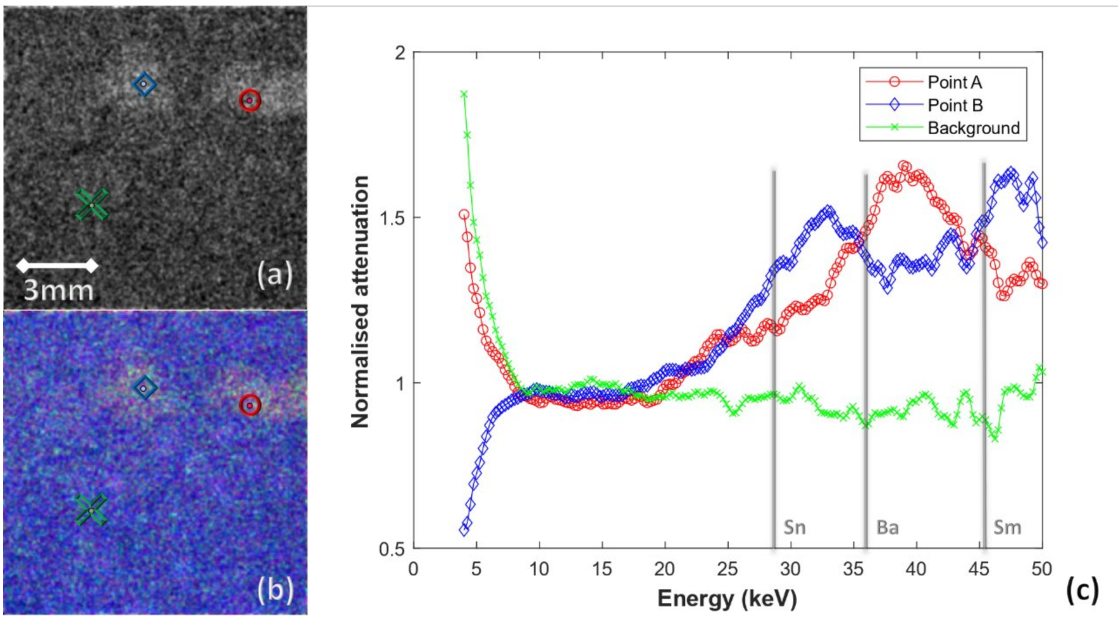

Supplementary Figure 5: Hyperspectral data: summed image (a), spectral band-coloured image (b) and spectrum at the dotted locations with a 3-pixels neighbourhood size (c)

Supplementary References

1. Soloviev VY, Renforth KL, Dirckx CJ, Wells SG. Meshless reconstruction technique for digital tomosynthesis. *Phys Med Biol* **65**, 085010 (2020).10.1088/1361-6560/ab7685

2. Soloviev VY, Wells SG, Renforth KL, Dirckx CJ. Metal artefact reduction in digital tomosynthesis using component decomposition. *Biomedical Physics & Engineering Express* **9**, 025003 (2023).10.1088/2057-1976/acb357

3. Jørgensen JS*, et al.* Core Imaging Library - Part I: a versatile Python framework for tomographic imaging. *Philosophical Transactions of the Royal Society A: Mathematical, Physical and Engineering Sciences* **379**, 20200192 (2021).doi:10.1098/rsta.2020.0192

4. van Aarle W*, et al.* The ASTRA Toolbox: A platform for advanced algorithm development in electron tomography. *Ultramicroscopy* **157**, 35-47 (2015).https://doi.org/10.1016/j.ultramic.2015.05.002

Figures